(2)

MTL TR 89-30

AD

STATISTICAL STRENGTH COMPARISON OF METAL-MATRIX AND POLYMERIC-MATRIX COMPOSITES

EDWARD M. WU
NAVAL POST GRADUATE SCHOOL

SHUN-CHIN CHOU
U.S. ARMY MATERIALS TECHNOLOGY LABORATORY
MATERIALS DYNAMICS BRANCH

April 1989

US ARMY
LABORATORY COMMAND
MATERIALS TECHNOLOGY LABORATORY

U.S. ARMY MATERIALS TECHNOLOGY LABORATORY
Watertown, Massachusetts 02172-0001

The findings in this report are not to be construed as an official Department of the Army position, unless so designated by other authorized documents.

Mention of any trade names or manufacturers in this report shall not be construed as advertising nor as an official indorsement or approval of such products or companies by the United States Government.

DISPOSITION INSTRUCTIONS

Destroy this report when it is no longer needed.
Do not return it to the originator

UNCLASSIFIED

SECURITY CLASSIFICATION OF THIS PAGE (When Data Entered)

REPORT DOCUMENTATION PAGE		READ INSTRUCTIONS BEFORE COMPLETING FORM
1. REPORT NUMBER MTL TR 89-30	2. GOVT ACCESSION NO.	3. RECIPIENT'S CATALOG NUMBER
4. TITLE (and Subtitle) STATISTICAL STRENGTH COMPARISON OF METAL-MATRIX AND POLYMERIC-MATRIX COMPOSITES		5. TYPE OF REPORT & PERIOD COVERED 6. PERFORMING ORG. REPORT NUMBER
7. AUTHOR(s) Edward M. Wu* and Shun-Chin Chou		8. CONTRACT OR GRANT NUMBER(s)
9. PERFORMING ORGANIZATION NAME AND ADDRESS U.S. Army Materials Technology Laboratory Watertown, Massachusetts 02172-0001 SLCMT-MRD		10. PROGRAM ELEMENT, PROJECT, TASK AREA & WORK UNIT NUMBERS D/A Project: 536-6010 P62322. K14A-2585 AMCMS Code: 69200R.897 A050
11. CONTROLLING OFFICE NAME AND ADDRESS U.S. Army Laboratory Command 2800 Powder Mill Road Adelphi, Maryland 20783-1145		12. REPORT DATE April 1989 13. NUMBER OF PAGES 19
14. MONITORING AGENCY NAME & ADDRESS(if different from Controlling Office)		15. SECURITY CLASS. (of this report) Unclassified 15a. DECLASSIFICATION/DOWNGRADING SCHEDULE

16. DISTRIBUTION STATEMENT (of this Report)

Approved for public release; distribution unlimited.

17. DISTRIBUTION STATEMENT (of the abstract entered in Block 20, if different from Report)

18. SUPPLEMENTARY NOTES

*Naval Postgraduate School, Monterey, California.
Published in Testing Technology of Metal Matrix Composites, ASTM STP 964, P. R. DiGiovanni and N. R. Adsit, Eds., American Society for Testing and Materials, Philadelphia, 1988, p. 104-120.

19. KEY WORDS (Continue on reverse side if necessary and identify by block number)

Statistical strength	Testing methods	Weibull distribution
Dimensional scaling	Filament testing	
Size effect	Metal matrix composites	

20. ABSTRACT (Continue on reverse side if necessary and identify by block number)

(SEE REVERSE SIDE)

DD FORM 1 JAN 73 1473 EDITION OF 1 NOV 65 IS OBSOLETE

UNCLASSIFIED

SECURITY CLASSIFICATION OF THIS PAGE (When Data Entered)

Block No. 20

ABSTRACT

The reliability of a composite structure depends on the materials strength variability. Unidirectional composites fail sequentially initiating from the very weakest fiber sites with matrix binder providing local redundancy by transferring load to neighboring fibers until cumulation and clustering of these sites lead to severe stress concentration and ultimate structure failure. As a consequence, the variability of the metal matrix structure is traceable to the strength variability of the constituent fiber, the metal matrix coating process, and the composite wire consolidation process. This report focuses on the partitioning of the first two sources of variability, identification and modeling of the dominant parameters, together with experimental measurement on a current graphite-aluminum composite. The statistical strength of several graphite spools are measured by testing single filament specimens at the beginning and at the end of the spools, thereby characterizing the statistical parameters associated with the strength variability among the spools and within each spool. The graphite-aluminum wire, produced from continuous liquid infiltration process are tested in tension. The metal matrix composite statistical strengths from different spools are compared with the respective statistical strength of the parent fiber. The results suggest that, given proper interpretation, single filament fiber strength is a sensitive parameter for quality assurance of metal matrix composites.

Edward M. Wu[1] *and S. C. Chou*[2]

Statistical Strength Comparison of Metal-Matrix and Polymeric-Matrix Composites

REFERENCE: Wu, E. M. and Chou, S. C., **"Statistical Strength Comparison of Metal-Matrix and Polymeric-Matrix Composites,"** *Testing Technology of Metal Matrix Composites, ASTM STP 964*, P. R. DiGiovanni and N. R. Adsit, Eds., American Society for Testing and Materials, Philadelphia, 1988, pp. 104–120.

ABSTRACT: The reliability of a composite structure depends on the materials strength variability. Unidirectional composites fail sequentially initiating from the very weakest fiber sites with matrix binder providing local redundancy by transferring load to neighboring fibers until cumulation and clustering of these sites lead to sever stress concentration and ultimate structure failure. As a consequence, the variability of the metal matrix structure is traceable to the strength variability of the constituent fiber, the metal matrix coating process, and the composite wire consolidation process. This report focuses on the partitioning of the first two sources of variability, identification and modeling of the dominant parameters, together with experimental measurment on a current graphite-aluminum composite. The statistical strength of several graphite spools are measured by testing single filament specimens at the beginning and at the end of the spools, thereby characterizing the statistical parameters associated with the strength variability among the spools and within each spool. The graphite-aluminum wire, produced from continuous liquid infiltration process are tested in tension. The metal matrix composite statistical strengths from differ spools are compared with the respective statistical strength of the parent fiber. The results suggest that, given proper interpretation, single filament fiber strength is a sensitive parameter for quality assurance of metal matrix composites.

KEY WORDS: statistical strength, dimensional scaling, size effect, testing methods, filament testing, metal matrix composites, Weibull distribution

Objective

The objective of this investigation is to perform experimental and analytical studies to:

1. Understand the failure process of metal matrix composites.
2. Identify the parametric roles of the fiber and the matrix which contribute to the *statistical* composite strength.

The results of this investigation will identify and quantify the attributes of metal matrix composites especially in comparison to polymeric composites. This understanding and characterization methodology discussed herein are relevant to:

(*a*) materials development and fabrication technology for metal matrix composites, and
(*b*) reliability design and quality assurance methodology for critical applications.

[1] Professor of Aeronautics, Department of Aeronautics, Naval Postgraduate School, Monterey, CA 93943.
[2] Army Materials Technology Laboratory, Watertown, MA 02172.

Background

Current PAN-based and pitch-based graphite fibers are achieving substantial improvement in strength largely through reduction of the fiber diameters. On the one hand, the smaller fiber diameter limits the maximum flaw size, thereby contributing to the strength increase. On the other hand, the smaller fiber approaches a geometrically true weakest-link-of-chain configuration, therefore causing a concurrent increase in variability. A strength scatter of 20 to 25% is not uncommon for current graphite fibers. Ordinarily, such high variability would render them unsuitable as an engineering structural material. However, the addition of a matrix binder causes a dramatic reduction in scatter to around 4% (for polymeric matrix composites).

The mechanism for the scatter reduction lies in the local structural redundancy provided by the matrix binder resulting in a sequential failure process rather than a catastrophic failure process. The sequential failure process is initiated by failure of weak fibers at very low load (as low as 15% of the ultimate load).

Through the adhesion of the matrix binder, the loads carried by these weak sites are transferred to neighboring fibers, thereby forestalling catastrophic failure of the entire composite. In fact these earlier fiber failures are not detectable except by acoustic emission detection instruments. Upon further load increase, more and more of the weak lower tail fibers fail leading to an increase in the spatial density of the failure sites and the companion increase in the probability of occurrence of *contiguous* failure sites. The contiguous fiber failure sites give rise to stress concentrations; the most severe of which causes ultimate catastrophic failure.

This sequential failure process caused by the micro-redundancy due to the presence of the matrix was qualitatively noted by Rosen [*1*], Zweben [*2*], and quantitatively modeled by Harlow and Phoenix [*3,4*], Phoenix and Smith [*5*]. The Harlow-Phoenix-Smith model predicts a reduction of strength scatter when fibers are bonded by a matrix binder in addition to the scatter reduction predicted by the Coleman's bundle theory. This is experimentally substantiated in Figs. 1*a* and 1*b* for graphite-epoxy composites. In Fig. 1*a*, the strength variability of the parent gaphite fibers were obtained by tension test of single filaments and presented in a linearized Weibull cumulative distribution function: $F^* = \ln(-\ln(1 - F))$ versus measured specimen strengths. The linear appearance of the data in this representation suggests a two parameter Weibull distribution model where the probability of failure is given by

$$F(\sigma) = 1 - \exp\{-(\sigma/\beta)^{\alpha}\} \tag{1}$$

where

σ = strength,
β = scale parameter (relatable to the mean strength), and
α = shape parameter (relatable to the variability) which is the slope in Fig. 1.

The good fit of the data to the Weibull model substantiates that the single filament fiber strength is well approximated by a weakest-link-of-chain process. From these data representations, we can observe (by noting the left-hand intercept of the curve with the ordinate) that at a stress level approximately 25% of mean strength (fiber stress 5 g), the probability of fiber failure is 10^{-3}. This is equivalent to a failure density of one fiber per cm^2 of a single layer of lamina [typically 0.0127 cm (.005 in.) thick]; a rather startling numbers of failures at such low stress level.

The scatter reducing effect of the matrix is demonstrated (in Fig. 1*b*) by the strength of graphite/epoxy composite strands, that is, epoxy impregnated tows of the same graphite

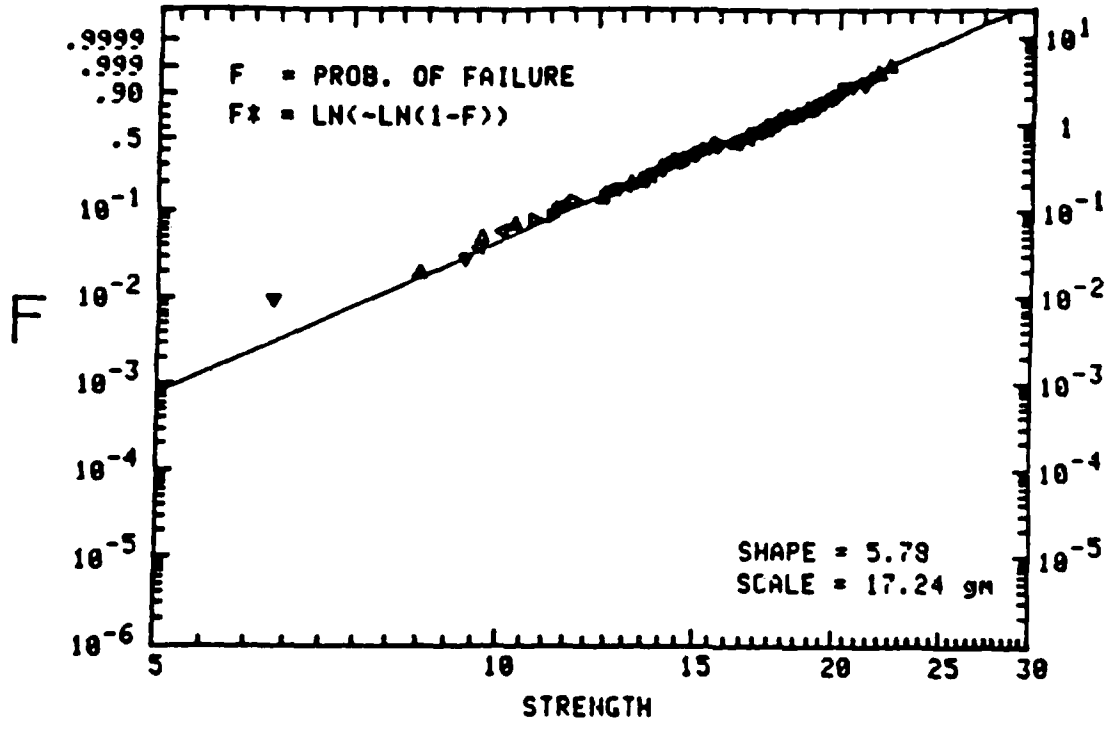

FIG. 1*a*—*Graphite fiber strength (force per fiber) with high variability, single filament without matrix binder.*

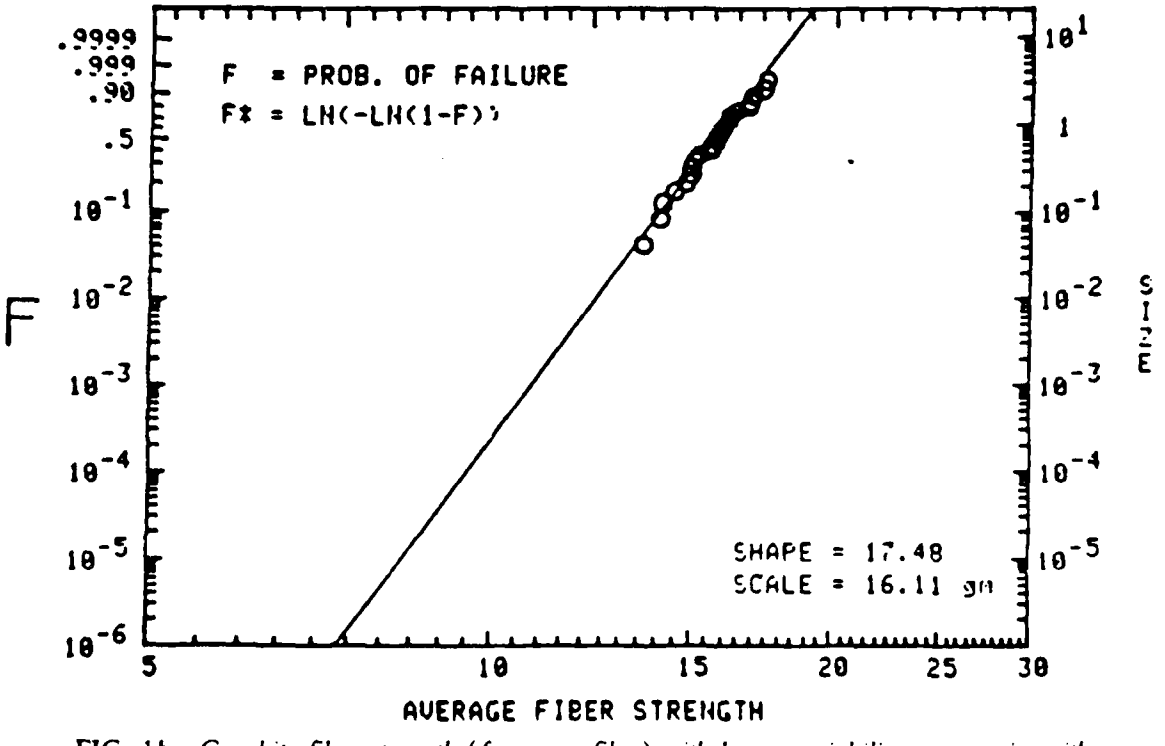

FIG. 1*b*—*Graphite fiber strength (force per fiber) with lower variability, composite with polymeric matrix binder.*

fiber. A dramatic reduction of variability can be observed through the slope increase (or rotation to vertical) of the strength distribution curve. As a result of this rotation, the probability of failure (at 25% mean stress) is reduced from 10^{-3} to 10^{-8}; a five orders of magnitude improvement as a result of the microredundancy provided by the matrix.

An important practical consequence of the strength variability is the strength dependency on the physical volume of a structure. The larger the volume, the higher the probability of encountering a fatal flaw, therefore the lower the mean strength. It follows that the larger the materials strength variability, the more severe the size effect. For the materials database presented in Figs. 1; given the fiber without matrix, an increase of physical size by 10^6 (that is, from a single layer 1 cm^2 lamina to 10 layer 3 m^2 laminate) would result in an expected decrease of mean strength by 90%! However, with this polymeric matrix, because of the reduction of scatter (the shape parameter α increases from 5.8 to 17.5), the expected decrease in mean strength (for the same size increase) is 45%. Table 1 summarizes the materials performance in the fiber form and that in the composite form with a polymeric matrix.

TABLE 1—*Materials performance in the fiber form and in the composite form with a polymeric matrix.*

Material	Scale, g	Shape	Mean, g	Coefficient of Variation, %
Fiber filament AS4	17.2	5.78	16	21
Fiber + polymer AS4 + DER332/T403	16.1	17.5	15.6	7

From this comparison, it is evident that high performance fibers can be a viable structure material only when used in conjunction with an effective matrix binder. The variability of composite and structure reliability in strength and life has been investigated by Phoenix and Wu [6]. The parametric roles of the statistical properties of the fiber and matrix and their interacted contribution to the composite properties must be *qualitatively* assessed. We can assess the dominating parameters through our understanding of the sequential failure process.

1. The demand on the matrix performance is inversely proportional to fiber variability. In the ideal limiting case where fiber strength has no variability, all fiber fail simultaneously, and no matrix load sharing will be needed.
2. The matrix effectiveness is proportional to the ratio of matrix-strength to fiber-strength (τ_m/σ_f) so that the load sharing can be maximized.
3. Matrix effectiveness is proportional to the ratio of matrix-shear modulus to fiber modulus (G_m/E_f) so that the ineffective length around the failure site can be minimized.
4. Matrix effectiveness is proportional to the ratio of matrix-ultimate strain to fiber-ultimate strain (ϵ_m/ϵ_f) so that stress singularity around the broken fiber will not be a catastrophic crack initiation site.

TABLE 2—*Typical values of dominating parameters for typical polymeric and aluminum matrices.*

Matrix Material	Matrix Strength τ_m / Fiber Strength σ_f	Matrix Shear Modulus G_m / Fiber Exterior Modulus E_f	Matrix Strain ϵ_m / Fiber Strain ϵ_f
Polymer	1/100	1/1000	2
Aluminum	1/50	1/5	4

We compare the typical values of these dominating parameters for typical polymeric matrix and aluminum matrix in Table 2.

From this comparison, we observed that aluminum matrix excels in all of the preceding strength governing parameters. We expect that, given the same fiber, aluminum should be more effective than polymer as a matrix binder material for high performance composites. We report on an experimental program to investigate the attributes of graphite-aluminum composites.

Experimental Program

The experimental program consists of selecting one spool of VSB64 pitch-base graphite fiber. Materials properties are listed in Appendix II and fabrication details are in accordance with standard ASTM practices. Specimens are sequentially made from the spool according to the following sequence starting from the beginning of the spool to the end of the spool:

1. Single filament fiber specimens.
2. Composite strand specimens with epoxy impregnation.
3. Composite wire specimens with aluminum impregnation.
4. Composite strand specimens with epoxy impregnation.
5. Single filament fiber specimens.

The statistical strength properties of the respective specimens were thoroughly charac-

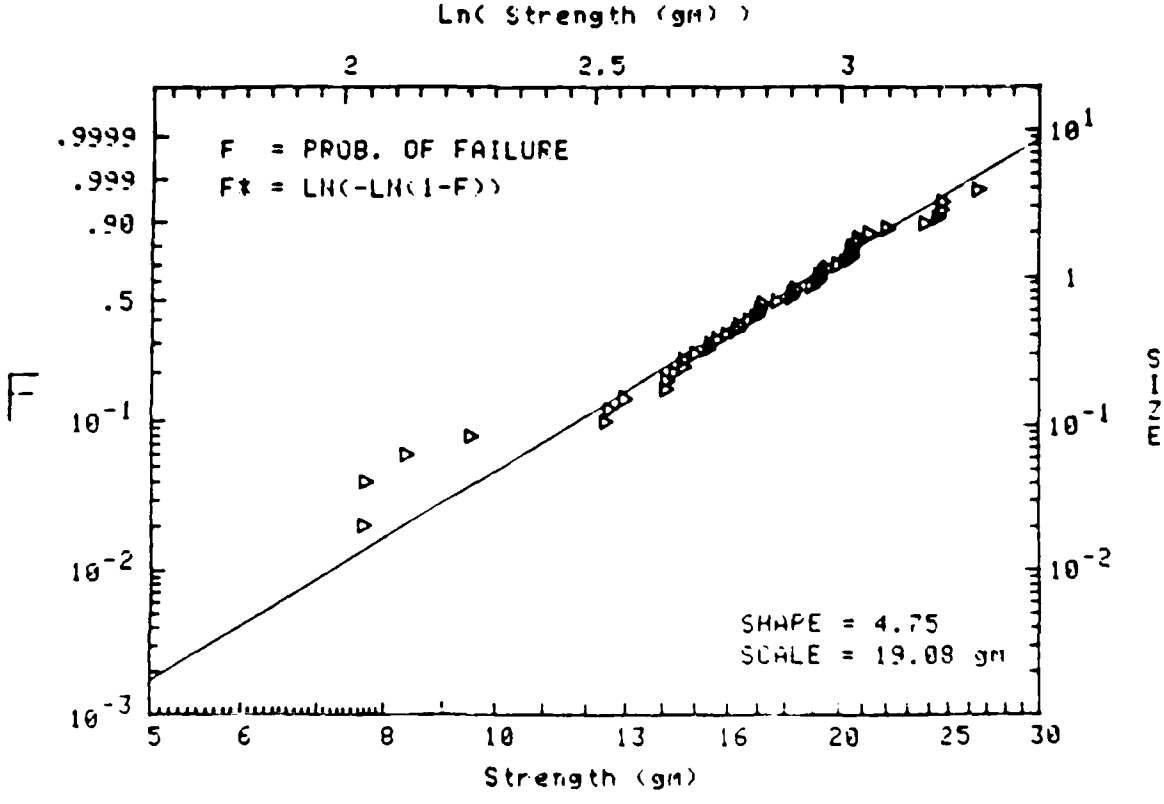

FIG. 2a—*Graphite fiber strength (force per fiber) single filament strength, specimen 1 from beginning of spool.*

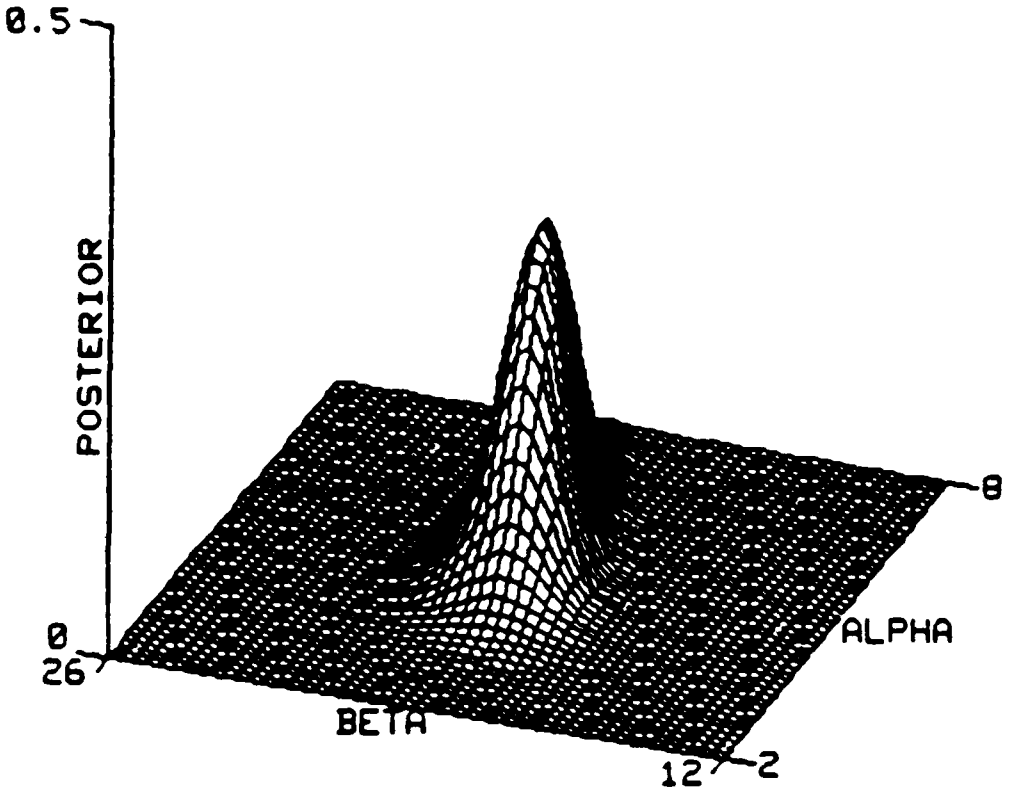

FIG. 2b—*Posterior density of the Weibull parameters* α,β *given data in Fig.* 2a.

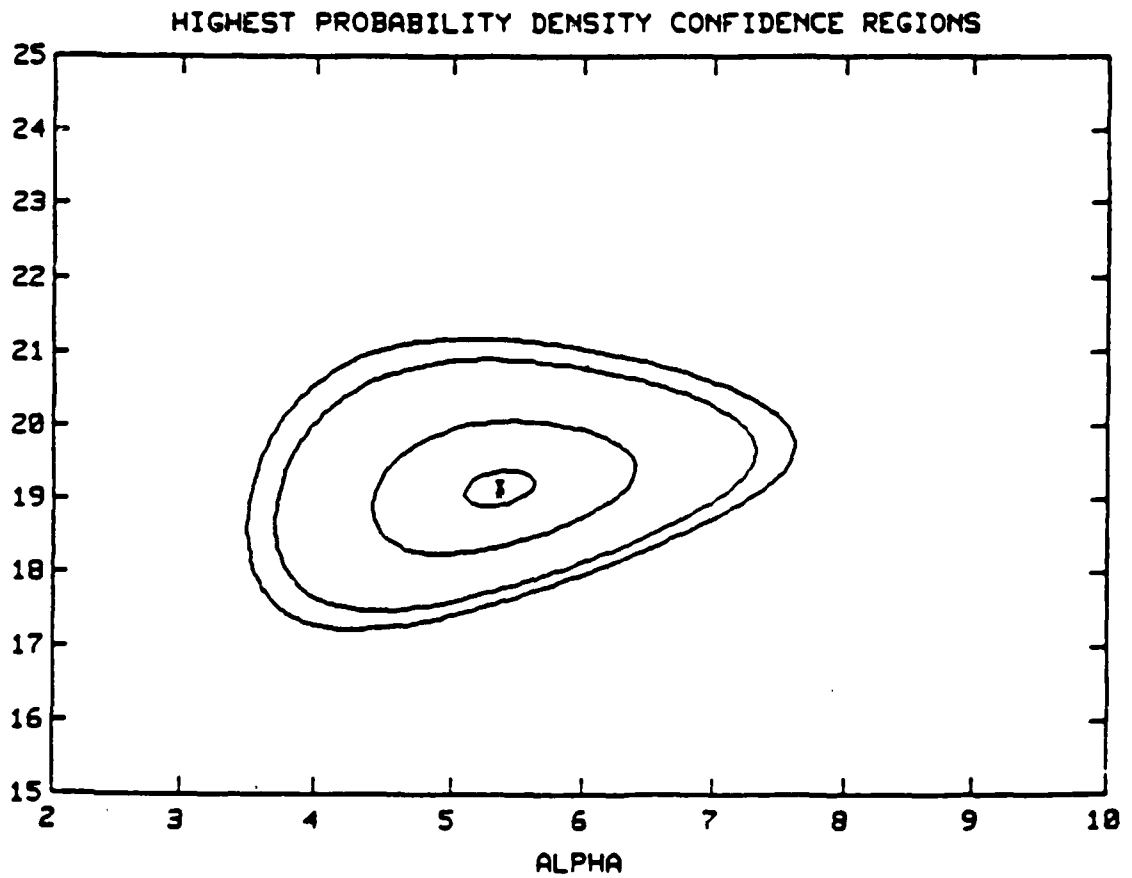

FIG. 2c—*Confidence contours of the Weibull parameters* α,β *given data in Fig.* 2a.

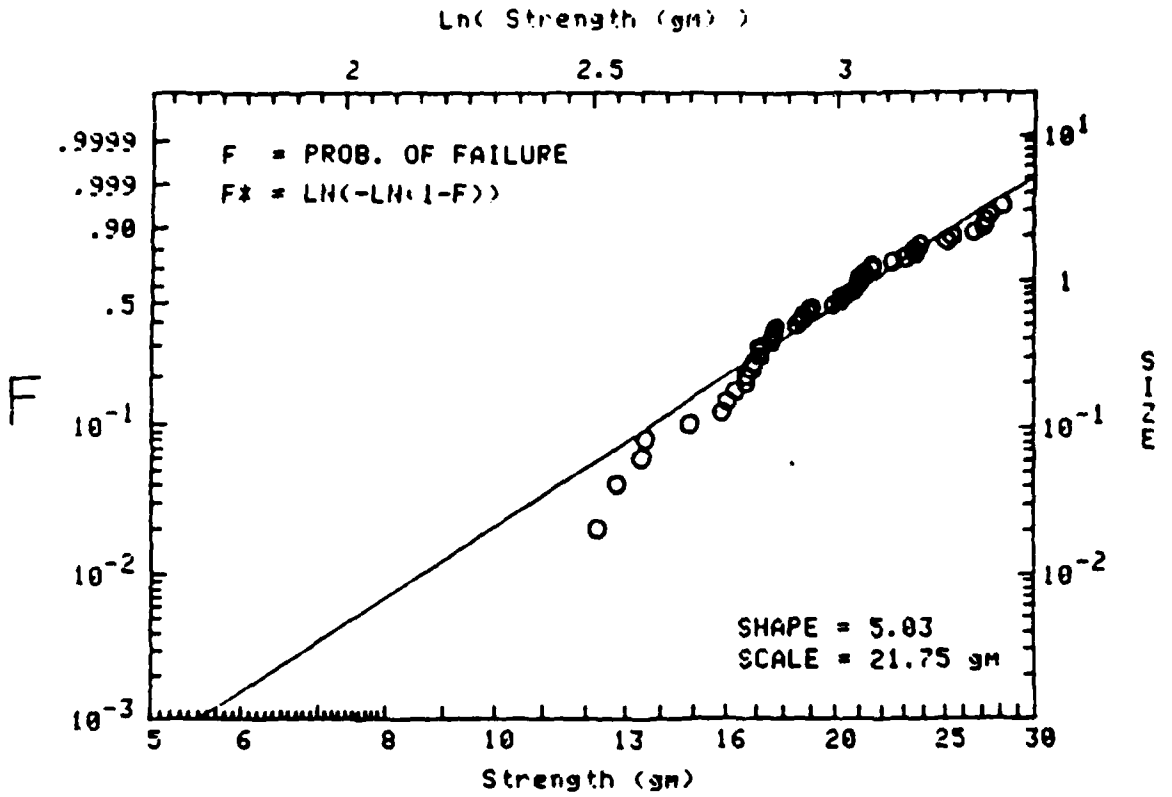

FIG. 3a—*Graphite fiber strength (force per fiber) single filament strength, specimen 5 from end of spool bracketing graphite/epoxy and graphite/aluminum composites for comparison.*

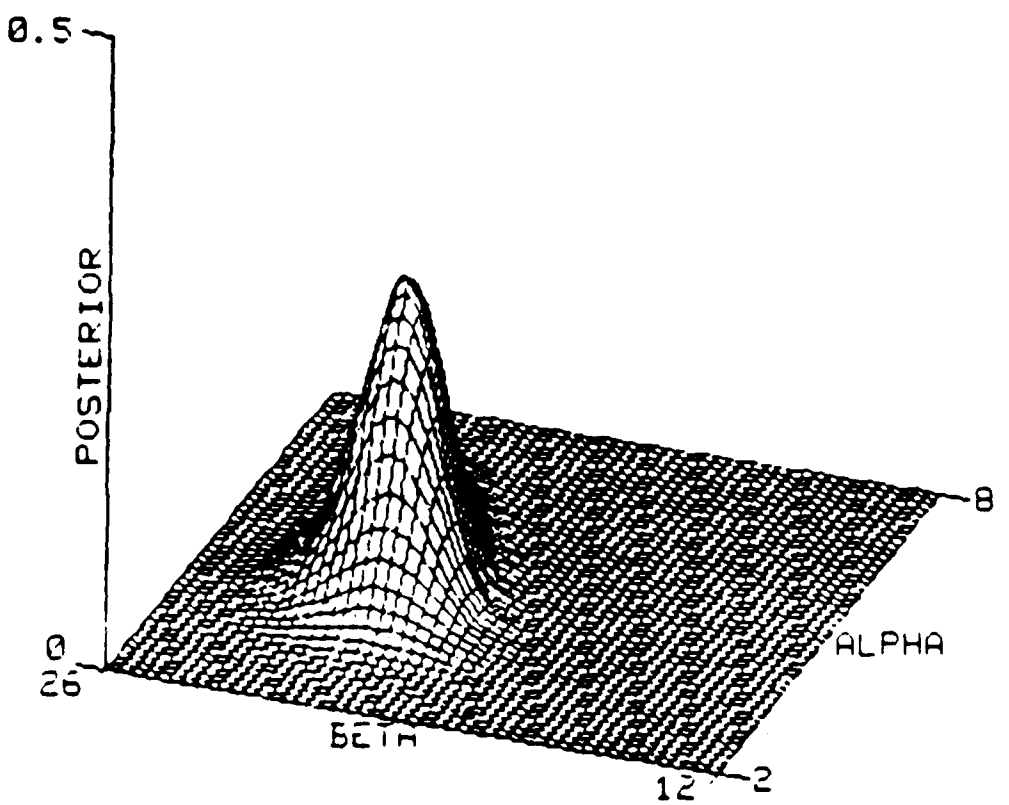

FIG. 3b—*Posterior density of the Weibull parameters α,β given data in Fig. 3a.*

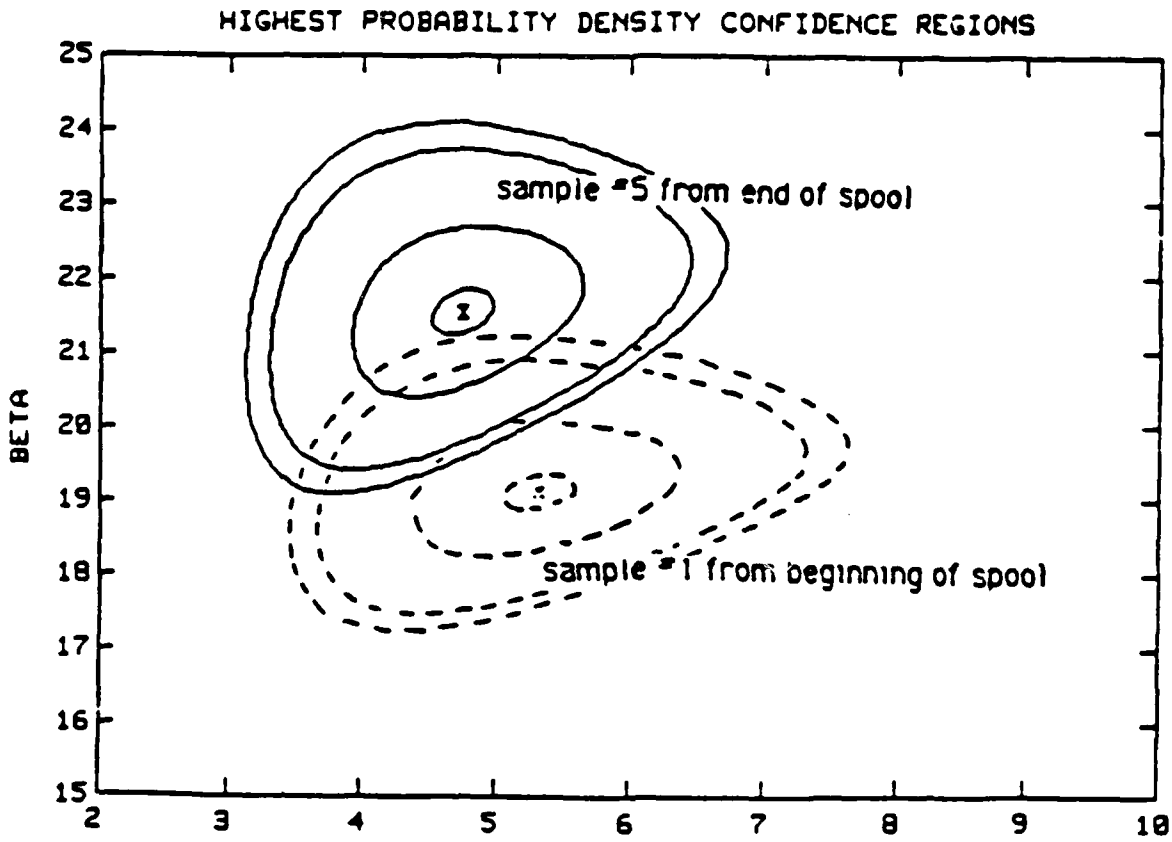

FIG. 3c—*Confidence contours of the Weibull parameters* α,β *given data in Fig.* 3a.

terized by tension test of an adequate number of specimens with respect to the observed scatter. That is, the number of test specimens are proportional to the variability observed. The testing methodology for each type of specimens are described in the Appendix I. This specimen allocation allows us to bracket the fiber strength variations within the spools so that an unambiguous relation between the graphite fibers and their composites can be established.

Results and Discussion

The results of the tension strength tests of each of the five specimen groups (as described in the "Experimental Program" section) are tabulated in Appendix III. From these data sets, we desired to examine the strength variability within the spool by comparing the strength at the beginning of the spool (data from Specimen 1) to the strength at the end of the spool (data from Specimen 5). If the strength variations are within the range of experimental resolution, we may infer that the constituent fibers in the composites Specimens 2, 3, and 4 are uniform and that they are from the same population. This would provide justification for merging data from Specimens 2 and 4 to form an unbiased representation of the graphite/epoxy composite strength.

This merged graphite/epoxy strength can be then compared to the graphite/aluminum strength from Specimen 3. Because of the statistical nature of the strength data such careful bracketing is necessitated in order to provide meaningful confidence level of the inferred conclusions.

In order to interpret the tabulated strength results we will select an appropriate statistical model, estimate the parameters of the model given the data from the respective specimens,

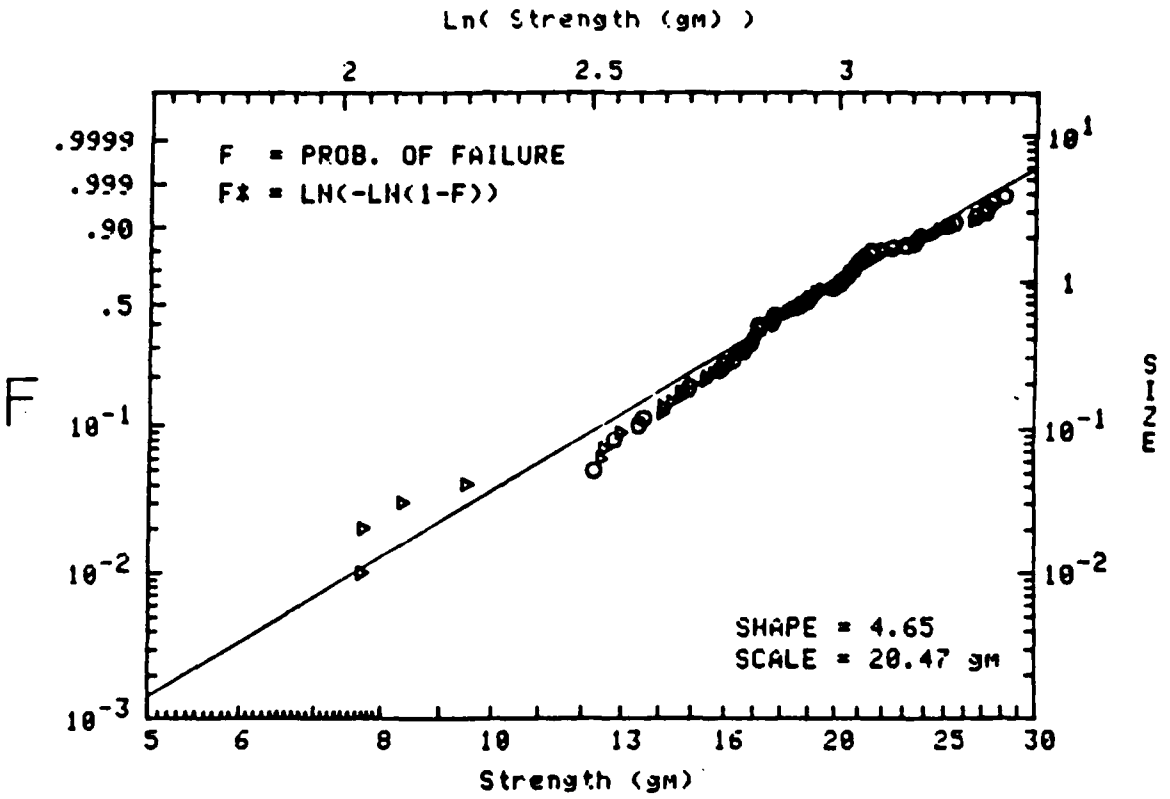

FIG. 4—*Graphite fiber strength (force per fiber) single filament strength, merged specimen 1 (beginning) and specimen 5 (end) of spool, bracketing benchmark for comparing the role of polymeric and metal matrix.*

then finally compare the parameters in accordance with the strategy outline previously. The two parameter Weibull model Eq 1 is selected to analyze the strength data. The selection is based on the physical failure process and substantiation by former experimental experiences (as described in the "Background" section). The shape α and scale β parameters for a given data specimen are obtained using the maximum likelihood estimator (MLE) numerically implemented based on the variable metric algorithm (BFGS) or the conjugated gradient algorithm (Beale). The confidence interval of the estimated parameter given a specimen data is calculated from Baye's formula

$$f(\alpha, \beta|D) = \frac{f(D|\alpha, \beta)f(\alpha, \beta)}{\int_{\alpha,\beta} f(D|\alpha, \beta)f(\alpha, \beta)\, d\alpha\, d\beta} \tag{2}$$

where

$f(\alpha, \beta|D)$ = posterior density given the data D,
$f(D|\alpha, \beta)$ = density of the data, and
$f(\alpha, \beta)$ is the prior density.

A flat prior $f(\alpha, \beta)$ = constant is used in all of the calculations herein.

Following the preceding procedure, the strengths of the fiber filament at the beginning of the spool (Specimen 1) are represented under linearized Weibull cumulative distribution

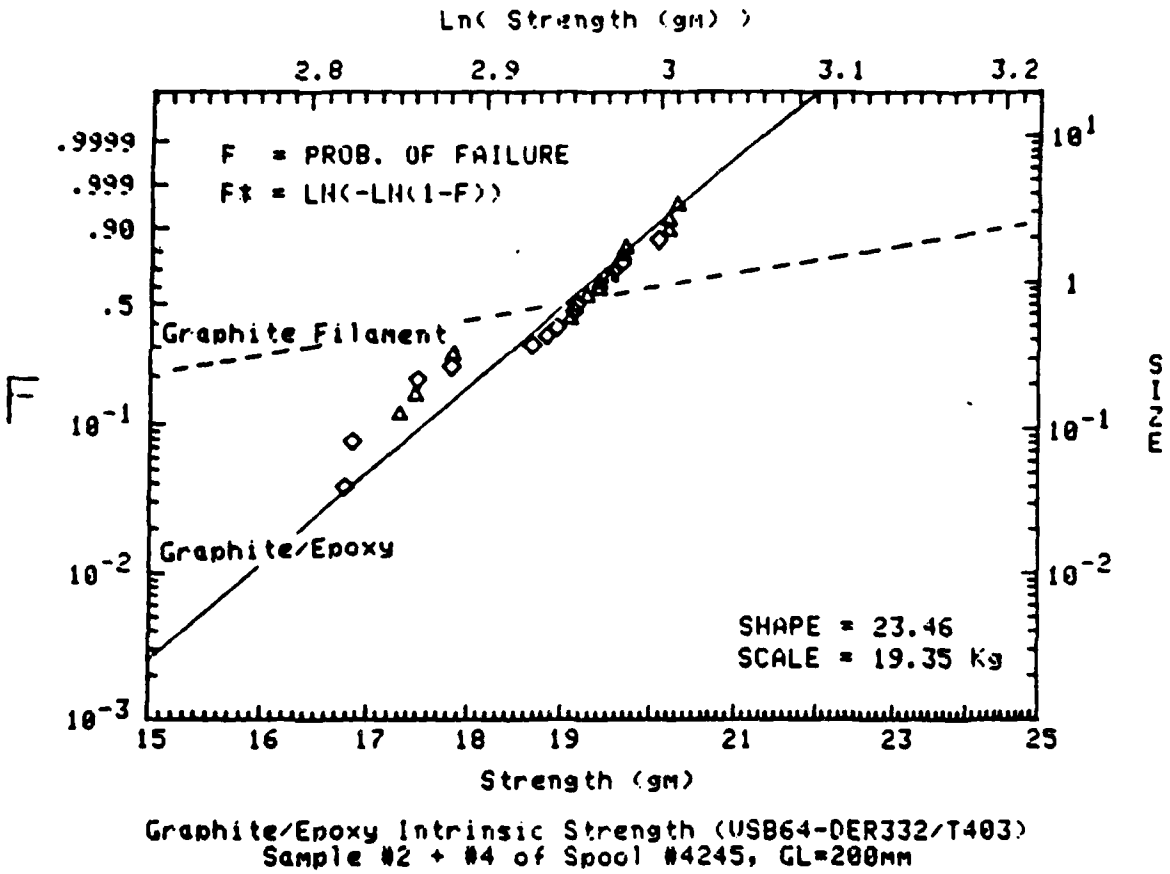

FIG. 5—*Graphite fiber strength (force per fiber) in graphite/epoxy composite, merged specimen 2 and specimen 4 bracketing graphite/aluminum composite. Scatter reduction is reflected by the vertical rotation.*

function and presented in Fig. 2*a*. We note, consistent with previous discussion, the large variation of the filament strength (indicated by $\alpha = 4.8$ or approximately a coefficient of variation of 25%). Figure 2*b* presents the posterior density of the parameters α, β. This density is a measure of the confidence of the parameter estimation given the current data set; the more peaky the density, the more confident the estimation. The equi-confidence contours of 5, 50, 90, and 95% of the posterior density function are presented in Fig. 2*c*. The interpretation of the 5% innermost contour is that the parameters measured by another specimen of equal size will have a 5% probability of lying within this contour.

The corresponding representation of the fiber filament data at the end of the spool (Specimen 5) are presented in Figs. 3*a*, 3*b*, and 3*c*. The dashed curves in these figures are transferred from (Specimen 1). Comparison of the numerical values of the shape α and scale β parameters (and also from cursory comparison between Fig. 2 and Fig. 3) suggests that the statistical strength of the fiber filament at the beginning and from the end of the spool are similar. This is confirmed by the Chi-square tests which indicated that there is over 50% probability that the two specimens are the same. It is therefore justified to merge Specimens 1 and 5 together to represent the statistical strength of the fiber filaments as presented in Fig. 4.

The graphite/epoxy data from Specimen 2 and Specimen 4 are interpreted in similar manner. They are inferred to be similar, and the two data sets are merged to form one combined data set which is presented in Fig. 5. Physically, it means that the two graphite/epoxy specimens which bracket the graphite/aluminum specimens belong strength-wise to

the same population. The dashed curve is transferred from the filament strength distribution (Fig. 4).

The graphite/aluminum data (Specimen 3) is in the center of the bracket and can be interpreted directly. The statistical strength of this graphite/aluminum composite is presented in Fig. 6. The dashed curves are transferred from Figs. 4 and 5 for comparison.

Interpretation

We collected a carefully planned and implemented data base of the parent fiber (Fig. 4), their graphite/epoxy composites (Fig. 5), and their aluminum composites (Fig. 6). For quantitative comparison, the respective value of the parameters are tabulated in Table 3.

We noted that current high performance graphite fibers have a natural high scatter and will have unavoidable early failures. This is observed and presented in Fig. 4. According to the physical failure process of composites, the role of the matrix binder is understood to provide local microredundancy around the early weak fiber failure sites. From Fig. 5, we note, consistent with the failure process, the epoxy matrix leads to a dramatic reduction of the scatter (α = 23.5 or a coefficient of variation of 5%).

From consideration of the parametric roles of stiffness, strength, and ultimate strain capacity, we surmise that aluminum could be a superior matrix material in comparison to polymeric matrix. The higher stiffness of aluminum minimizes the zone of load sharing (the

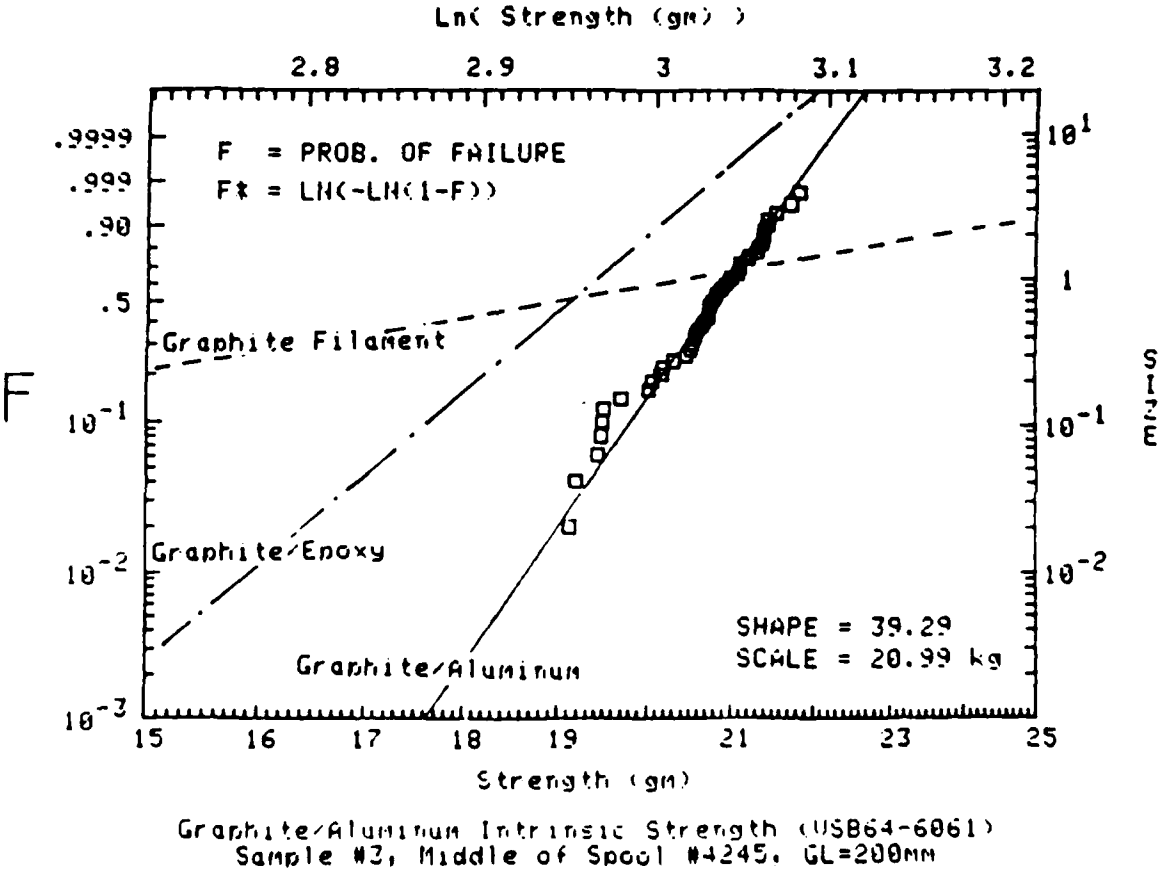

FIG. 6—*Graphite fiber strength (force per fiber) in graphite/aluminum composite specimen 3, bracketed by graphite/epoxy composite specimens (2 and 4) and single filament specimens (1 and 5). Scatter reduction is reflected by the vertical rotation; strength increase is reflected by the right shift.*

TABLE 3—*Respective values of the polymers.*

Materials	Scale, β (g)	Shape, α	Mean, μ (g)	Coefficent of Variation, cv
Fiber filament	20.4	4.6	19	26
Graphite/epoxy	19.4	23.5	18	5
Graphite/aluminum	21.0	39.3	21	3

ineffective length). The higher strength maximizes the magnitude of load sharing. The higher ultimate strain capacity increases the fracture toughness around the stress singularity of broken fiber end. Figure 6 confirms that aluminum leads to an even greater reduction of scatter (α = 39.3 or coefficient of variation of 3%).

Conclusions and Recommendations

This investigation identified and quantified the role of aluminum matrix in reducing strength scatter. This attribute of metal matrix is not generally recognized. It is of great practical importance in reducing strength dependence on the size (or volume) of a structure. A shape parameter change from 20 to 40 will result in a minimization of strength reduction by 250%. In other words, it is feasible to build large graphite aluminum structures with high structural efficiency (higher stress) *and* high reliability.

The results of this investigation suggest additional explorations in the following areas:

1. Strength size effect.
2. Stress singularity around broken fiber tip in the presence of matrix with plasticity.

Acknowledgment

This work was performed under the auspices of the U.S. Army, Materials Technology Laboratory, under BMD Materials, program manager, John Dignam.

References

[1] Rosen, B. W., "Tensile Failure of Fiberous Composites," *AIAA Journal*, American Institute of Aeronautics and Space Administration, Vol. 2, 1964, pp. 1985–1991.

[2] Zweben, C. and Rosen, B. W., "A Statistical Theory of Material Strength with Application to Composite Materials," *Journal of the Mechanics and Physics of Solids*, Vol. 18, 1970, pp. 189–206.

[3] Harlow, D. G. and Phoenix, S. L., "The Chain-of-Bundles Probability Model for Strength of Fibrous Materials I: Analysis and Conjectures," *Journal of Composite Materials*, Vol. 12, 1978, pp. 195–214.

[4] Harlow, D. G. and Phoenix, S. L., "The Chain-of-Bundles Probability Model for Strength of Fibrous Materials II: A Numerical Study of Convergence," *Journal of Composite Materials*, Vol. 12, 1978, pp. 314–334.

[5] Phoenix, S. L. and Smith, R. L., "A Comparison of Probabilistic Techniques for the Strength of Fiberous Materials Under Local Load-Sharing Among Fibers," *International Journal of Solids Structures*, Vol. 19, No. 6, 1983, pp. 479–496.

[6] Phoenix, S. L. and Wu, E. M., "Statistics for the Time Dependent Failure of Kevlar-49/Epoxy Composites: Micromechanical Modeling and Data Interpretation," *Mechanics of Composite Materials-Recent Advances*, Hashin and Herakovich, Eds. Pergamon Press, Elmsford, N.Y., 1982, pp. 135–162.

APPENDIX I

Experimental Method of Graphite-aluminum Tension Test

This appendix describes the experimental methods for measuring the tensile strength of graphite-aluminum composites. The specimen configuration considered herein is that of a strand (wire) which is a matrix impregnated tow of graphite fibers. Specifically in this investigation, the matrix is 6061 aluminum and the tow consists of 1000 fiber ends. The constituent properties of the fiber and the matrix are listed in Appendix II. The composite wire is nominally straight as fabricated, and multiple wires can be consolidated into tapes which can in turn be consolidated into laminae, then laminates, finally, the end structure. Hence, the composite wire may be considered as the primary building block for graphite aluminum structures. A proper characterization of the strength properties of the wire is the basis for quantitatively assessing material process development and ultimately for predicting the strength and reliability of the end composite structure. For such purposes, the pertinent strength properties include: the mean, the variability, and the strength dependency on the size (volume) of the specimen.

Tensile Strength Properties Are Measured in This Investigation

Tension testing of composites is simple in concept but difficult in experimental implementation. In tension testing of homogeneous material, a specimen configuration of reduced cross section within the gage length (the "dog-bone" configuration) can be used to reduce the stress in the gripping region and to assure a uniform tension state of stress within the gage section. As a result, evaluation of each individual test datum is straightforward. Those with failure sites within the gage length are valid tests, and any strength variation within the valid test can be accepted as the characteristic of the material. Those with failure sites outside the gage length can be discarded with assurance that the underlying materials characteristic will not be biased.

However, for heterogeneous composites, the reduced cross-section solution is not always applicable. In fiber reinforced composites, the stiff fibers carry the primary portion of the load, and the transfer of the gripping force (which is in shear) to the interior fibers depends on the shear transfer ability of the matrix. The complex state of stress in the grip area increases the likelihood of failure in the grip vicinity therefore does not provide the representative strength value. On the other hand, identification and censoring of these specimens are not straightforward. For a specimen of slender configuration under tension, propagation of stress wave initiated from the failure site causes multiple secondary failures sites breaking the specimen into many segments rendering the identification of the original failure site exceeding difficult and uncertain. In this investigation, we developed experimental methods to:

1. Increase the shear transfer capacity of the adhesive between the grip and the specimen.
2. Increase the shear transfer capacity of the matrix in the neighborhood of the grip.
3. Protect the specimen from fragmentation by the failure initiated stress wave, thereby allowing positive identification whether failure initiated around the grip vicinity and unambiguously accept or censor a specific test datum.

Gripping Method of Composite Wire Specimen

Conventional method of load introduction by adhesive bonding of the specimen to a tab has two limitations. The first limitation is that there exist a high shear stress concentration where the tab terminates toward the gage section, this lead to adhesive failure and loss of

definition of the gage dimension. The second limitation is that the applied tension from the testing machine is transferred through shear of the adhesive into the specimen which in turn transfers via shear of the matrix into tensile load of the fiber. The shear stress is maximum at the bonding adhesive and decreases to zero at the interior center of the specimen. This nonuniform stress distribution gives rise to a tension peeling stress at the edge of the tab and specimen interface. Such peeling tension stress is known to severely reduce the adhesive strength.

To overcome these limitations, we developed a tubular tab to fully enclose the wire. The tubular tab is made of thin-walled copper tubing with an internal diameter to give nominal 0.01 mm (.004 in.) diametrical clearance with the wire. Prior to bonding to the specimen the copper tube is annealed and de-scaled in an acid bath. Graphite/aluminum wire specimens are cut to length with diameters and the weight measured and recorded. Appropriate fixtures are designed to assure the concentric alignment of the tubular tab and the wire specimen at the proper gage location. An anaerobic adhesive is injected into the space between the tubular tab and specimen and allowed to set. Specimens are now ready for tension testing.

For measuring the intrinsic strength (that is, the short time static strength) of the composite wire, chucks (commercially available for jeweler's lathe) are mounted to a universal tension testing machine with precision alignment to minimize any bending. Special jaws are sized for tubular tab such that when the jaws are fully tightened in the chuck, the tubular tabs are subjected to a 1.5% diametrical strain. Since the jaw reduces tab diameter uniformly, a state of hydrostatic compression strain is applied to the specimen and adhesive in the bonding region. This state of hydrostatic strain is retained by the strain hardening action of the copper tubing. This hydrostatic strain provides two important functions:

1. The hydrostatic stress simultaneously cancels the tension peel stress and increases the strength of the adhesive.
2. The hydrostatic stress is uniformly transferred to the composite and increases the shear strength of the matrix.

The combination of these two functions leads to minimization of failure in the grip vicinity to less than 5% of the specimens tested.

APPENDIX II

Constituent Properties of Fiber and Matrix

Fiber Properties	
Manufacturer	Union Carbide Corporation
Type	Pitch Based Graphite (VSB-64)
Modulus E_f	55 Msi
Diameter	10 μm
Density	0.072 lb/in.^{3}
Bundle (tow)	1000
Matrix Properties	
Aluminum	
Type	6061-F condition, T-4 estimated
Modulus E_m	10 Msi (69 GPa)
Shear Modulus G_m	3.8 Msi (26 GPa)
Yield τ_{yield}	27 ksi (0.19 GPa) estimated
Fiber volume V_f	46% (nominal)

Appendix Ii—*Continued.*

Epoxy	
Type	DER-332/T403[a]
Modulus E_m	0.48 Msi (3.3 GPa)
Shear Modulus G_m	0.16 Msi (1.1 GPa)
Yield τ_{yield}	11.5 ksi (0.079 GPa) estimated
Fiber volume V_f	55% (nominal)

[a] A bisphenol-A-based epoxy resin (Dow Chemical: DER-332) cured with an aliphatic polyether triamine (Jefferson Chemical: Jeffamine T403). The stoichiometric ratio of resin to curing agent is 55/45 by weight, cured at 60°C for 16 h.

APPENDIX III

Tabulation of Ordered Tensile Strength of Specimens 1, 2, 3, 4, and 5

Graphite filament intrinsic strength (VSB64-pitch) Specimen 1, beginning of Spool 4245, GL = 50 mm.

No.	Strength, g	Code	No.	Strength, g	Code
1	7.680	1.	26	18.170	1.
2	7.700	1.	27	18.230	1.
3	8.340	1.	28	18.360	1.
4	9.490	1.	29	18.940	1.
5	12.440	1.	30	19.120	1.
6	12.540	1.	31	19.200	1.
7	12.950	1.	32	19.200	1.
8	14.080	1.	33	19.370	1.
9	14.110	1.	34	19.500	1.
10	14.330	1.	35	19.960	1.
11	14.590	1.	36	20.220	1.
12	14.630	1.	37	20.450	1.
13	14.950	1.	38	20.480	1.
14	15.360	1.	39	20.480	1.
15	15.400	1.	40	20.540	1.
16	15.650	1.	41	20.730	1.
17	15.910	1.	42	20.790	1.
18	16.290	1.	43	21.250	1.
19	16.350	1.	44	22.000	1.
20	16.680	1.	45	23.740	1.
21	16.930	1.	46	24.380	1.
22	17.020	1.	47	24.580	1.
23	17.060	1.	48	24.640	1.
24	17.150	1.	49	26.490	1.
25	17.660	1.			

NOTE—
Two-parameter Weibull distribution maximum likelihood estimates.
Shape parameter = 4.7458.
Scale parameter = 19.0846 g.
49th root of maximum likelihood function = 0.0577.
0-points progressively censored.

Graphite/epoxy intrinsic strength (VSB64-DER332/T403) Specimen 2, beginning of Spool 4245, GL = 200 mm.

No.	Strength, kg	Code	No.	Strength, kg	Code
1	17.300	4.	8	19.530	4.
2	17.470	4.	9	19.650	4.
3	17.840	4.	10	19.690	4.
4	19.080	4.	11	20.190	4.
5	19.260	4.	12	20.190	4.
6	19.390	4.	13	20.290	4.
7	19.400	4.			

NOTE—
Two-parameter Weibull distribution maximum likelihood estimates.
Shape parameter = 27.3933.
Scale parameter = 19.5971 kg.
13th root of maximum likelihood function = 0.2797.
0-points progressively censored.

Graphite/aluminum intrinsic strength (VSB64-6061) Specimen 3, middle of Spool 4245, GL = 200 mm.

No.	Strength, kg	Code	No.	Strength, kg	Code
1	19.120	8.	26	20.800	8.
2	19.180	8.	27	20.810	8.
3	19.430	8.	28	20.860	8.
4	19.460	8.	29	20.890	8.
5	19.480	8.	30	20.930	8.
6	19.500	8.	31	20.970	8.
7	19.700	8.	32	20.990	8.
8	20.020	8.	33	21.070	8.
9	20.060	8.	34	21.080	8.
10	20.160	8.	35	21.100	8.
11	20.180	8.	36	21.100	8.
12	20.310	8.	37	21.180	8.
13	20.460	8.	38	21.210	8.
14	20.520	8.	39	21.300	8.
15	20.530	8.	40	21.320	8.
16	20.550	8.	41	21.360	8.
17	20.570	8.	42	21.370	8.
18	20.600	8.	43	21.390	8.
19	20.640	8.	44	21.390	8.
20	20.670	8.	45	21.430	8.
21	20.710	8.	46	21.440	8.
22	20.720	8.	47	21.530	8.
23	20.730	8.	48	21.710	8.
24	20.740	8.	49	21.810	8.
25	20.770	8.			

NOTE—
Two-parameter Weibull distribution maximum likelihood estimates.
Shape parameter = 39.2892.
Scale parameter = 20.9907 kg.
49th root of maximum likelihood function = 0.3890.
0-points progressively censored.

Graphite/epoxy intrinsic strength (VSB64-DER332/T403) Specimen 4, end of Spool 4245, GL = 200 mm.

No.	Strength, kg	Code	No.	Strength, kg	Code
1	16.780	5.	7	18.930	5.
2	16.850	5.	8	19.120	5.
3	17.490	5.	9	19.150	5.
4	17.830	5.	10	19.560	5.
5	18.660	5.	11	19.640	5.
6	18.820	5.	12	20.060	5.

NOTE—
Two-parameter Weibull distribution maximum likelihood estimates.
Shape parameter = 22.3987.
Scale parameter = 19.0453 kg.
12th root of maximum likelihood function = 0.2445.
0-points progressively censored.

Graphite filament intrinsic strength (VSB64-pitch) Specimen 5, end of Spool 4245, GL = 50 mm.

No.	Strength, g	Code	No.	Strength, g	Code
1	12.280	9.	26	20.180	9.
2	12.800	9.	27	20.220	9.
3	13.440	9.	28	20.480	9.
4	13.570	9.	29	20.730	9.
5	14.870	9.	30	20.860	9.
6	15.870	9.	31	21.000	9.
7	16.040	9.	32	21.000	9.
8	16.290	9.	33	21.050	9.
9	16.640	9.	34	21.180	9.
10	16.680	9.	35	21.500	9.
11	16.890	9.	36	21.500	9.
12	16.930	9.	37	22.460	9.
13	17.150	9.	38	23.040	9.
14	17.150	9.	39	23.480	9.
15	17.150	9.	40	23.480	9.
16	17.570	9.	41	23.740	9.
17	17.610	9.	42	25.080	9.
18	17.650	9.	43	25.400	9.
19	17.700	9.	44	26.620	9.
20	18.480	9.	45	27.130	9.
21	18.610	9.	46	27.210	9.
22	18.680	9.	47	27.460	9.
23	18.860	9.	48	28.160	9.
24	18.990	9.	49	30.540	9.
25	19.890	9.			

NOTE—
Two-parameter Weibull distribution maximum likelihood estimates.
Shape parameter = 5.0262.
Scale parameter = 21.7505 g.
49th root of maximum likelihood function = 0.0558.
0-points progressively censored.

DISTRIBUTION LIST

No. of Copies	To
	Office of Deputy Under Secretary of Defense for Research and Engineering, The Pentagon, Washington, DC 20301
1	ATTN: J. Persh, Staff Specialist for Materials and Structures (Room 3D1089)
	Office of Deputy Chief of Research, Development and Acquisition, The Pentagon, Washington, DC 20301
1	ATTN: DAMA-CSS
	Commander, U.S. Army Laboratory Command, 2800 Powder Mill Road, Adelphi, MD 20783-1145
1	ATTN: AMSLC-TD, Office of the Technical Director
	Commander, U.S. Army Materiel Command, 5001 Eisenhower Avenue, Alexandria, VA 22333-0001
1	ATTN: AMCLD
1	AMCSCI, Dr. Chait (Room 10E20)
	Strategic Defense Initiative Office, The Pentagon, Washington, DC 20304
1	ATTN: SLKT, Major R. Yesensky
1	SLKT, A. Young
	Director, U.S. Strategic Defense Command, P.O. Box 1500, Huntsville, AL 35807-3801
1	ATTN: CSSD-H-QX, D. Bouska
1	CSSD-H-LK, L. Atha
1	CSSD-H-LK, L. Cochran
1	CSSD-H-HA, R. Buckelew
1	CSSD-H-E, J. Katechis
1	CSSD-H-Q, E. Wilkinson
1	CSSD-H-Q, R. Riviera
1	CSSD-H-QE, J. Papadopoulos
	Commander, U.S. Army Missile Command, Redstone Arsenal, Huntsville, AL 35809
1	ATTN: AMSMI-EAM, P. Ormsby
	Commander, U.S. Army Combat Development Command, Institute of Nuclear Studies, Fort Bliss, TX 79916
1	ATTN: Technical Library
	Commander, Naval Surface Warfare Center, Silver Springs, MD 20910
1	ATTN: J. Foltz
	Commander, U.S. Air Force Wright Aeronautical Laboratories, Wright-Patterson Air Force Base, OH 45433
1	ATTN: AFWAL/FIBAA, A. Gunderson
1	AFWAL/FIBAA, C. R. Waitz
1	AFWAL/MLLS, T. Ronald

No. of Copies	To
	Commander, BMO/ASMS, Norton Air Force Base, CA 92409
1	ATTN: Capt. T. Williams
	Director, Defense Nuclear Agency, Washington, DC 20305-1000
1	ATTN: B. Gillis
	Commander, Defense Technical Information Center, Cameron Station, Building 5, 5010 Duke Street, Alexandria, VA 22304-6145
2	ATTN: DTIC-FDAC
	National Aeronautics and Space Administration, Langley Research Center, Hampton, VA 23665
1	ATTN: W. Brewer, Code MS-224
	Institute for Defense Analysis, 1801 N. Beauregard Street, Alexandria, VA 22311
1	ATTN: M. Rigdon
	Aerospace Corporation, P.O. Box 92957, Los Angeles, CA 90009
1	ATTN: L. McCreight
1	H. Katzman
	AVCO Systems Division of Textron, Inc., 201 Lowell Street, Wilmington, MA 01887
1	ATTN: V. DiCristina
	AVCO Specialty Materials, Subsidiary of Textron, Inc., 2 Industrial Avenue, Lowell, MA 01851
1	ATTN: P. Hoffman
1	M. Mittnick
	The Boeing Aerospace Company, P.O. Box 3999, Seattle, WA 98124
1	ATTN: S. Bigelow
1	P. G. Rimbos
1	B. K. Das
1	T. Luhman
	Charles Stark Draper Laboratories, 555 Technology Avenue, Cambridge, MA 02139
1	ATTN: J. Gubbay
	DWA Composite Specialties, Inc., 21133 Superior Street, Chatsworth, CA 91311
1	ATTN: J. F. Dolowy, Jr.
	Fiber Materials, Inc., Biddeford Industrial Park, Biddeford, ME 04005
1	ATTN: R. Burns
	General Dynamics Corporation, Convair Division, P.O. Box 80847, San Diego, CA 92130
1	ATTN: J. Hertz
1	K. Meyer

No. of Copies	To
	General Electric Company, Advanced Materials Development Laboratory, 3198 Chestnut Street, Philadelphia, PA 19101
1	ATTN: J. Brazel
1	K. Hall
	General Electric Company, Valley Forge Space Center, P.O. Box 8555, Philadelphia, PA 19101
1	ATTN: C. Zweben
	General Research Corporation, P.O. Box 6770, 5383 Hollister Avenue, Santa Barbara, CA 93111
1	ATTN: J. Green
	Kaman Tempo, 816 State Street, Santa Barbara, CA 93101
1	ATTN: L. Gonzalez
	Lockheed-Georgia Company, 86 South Cobb Drive, Marietta, GA 30063
1	ATTN: J. Carrol
1	W. Bates
	Lockheed Missile and Space Company, 1111 Lockheed Way, Sunnyvale, CA 94089
1	ATTN: W. Loomis
1	D. Himmelblau
1	R. Torczyner
1	H. Chang
	Martin Marietta Orlando Aerospace, P.O. Box 5837, Orlando, FL 32085
1	ATTN: R. Caime
1	K. Hanson
1	F. Koo
1	M. Hendricks
	Martin Marietta Baltimore Aerospace, 103 Chesapeake Park Plaza, Baltimore, MD 21220
1	ATTN: W. Couch
	Martin Marietta Denver Aerospace, P.O. Box 179, Denver, CO 80201
1	ATTN: M. Misra
	Material Concepts, Inc., 666 North Hague Avenue, Columbus, OH 43204
1	ATTN: D. Kizer
	McDonnell Douglas Astronautics Company, 5301 Bolsa Avenue, Huntington Beach, CA 92647
1	ATTN: J. Ditto
1	J. Davidson
1	J. Grossman
1	H. Parachanian
1	B. Leonard

No. of Copies	To
	PDA Engineering, 2975 Red Hill Avenue, Costa Mesa, CA 92626
1	ATTN: M. Sherman
	Rohr Industries, Inc., Foot of H Street, P.O. Box 878, Chula Vista, CA 92012-0878
1	ATTN: N. R. Adsit
	SPARTA, Inc., 1055 Wall Street, Suite 200, P.O. Box 1354, La Jolla, CA 92038
1	ATTN: J. Glatz
1	G. Wonacott
	SPARTA, Inc., 3440 Carson Street, Suite 300, Torrance, CA 90503
1	ATTN: I. Osofsky
	SPARTA, Inc., 1104B Camino Del Mar, Del Mar, CA 92014
1	ATTN: D. Weisinger
	Southwest Research Institute, 8500 Culebra Road, San Antonio, TX 78206
1	ATTN: A. Wenzel
	Stone Engineering Company, 805 Madison Street, Suite 2C, Huntsville, AL 35801
1	ATTN: W. Stone
	Teledyne Brown Engineering, Research Park, 300 Sparkman Drive, Huntsville, AL 35807
1	ATTN: C. Patty
	Director, U.S. Army Materials Technology Laboratory, Watertown, MA 02172-0001
2	ATTN: SLCMT-TML
2	Authors

U.S. Army Materials Technology Laboratory, Watertown, Massachusetts 02172-0001
STATISTICAL STRENGTH COMPARISON OF METAL-MATRIX AND POLYMERIC-MATRIX COMPOSITES -
Edward M. Wu and Shun-Chin Chou

Technical Report MTL TR 89-30, April 1989, 19 pp - illus-tables, D/A Project 536-6010 P62322. K14A-2585, AMCMS Code 69200R.897 A050

AD ____________

UNCLASSIFIED
UNLIMITED DISTRIBUTION

Key Words

Statistical strength
Dimensional scaling
Size effect

The reliability of a composite structure depends on the materials strength variability. Unidirectional composites fail sequentially initiating from the very weakest fiber sites with matrix binder providing local redundancy by transferring load to neighboring fibers until cumulation and clustering of these sites lead to severe stress concentration and ultimate structure failure. As a consequence, the variability of the metal matrix structure is traceable to the strength variability of the constituent fiber, the metal matrix coating process, and the composite wire consolidation process. This report focuses on the partitioning of the first two sources of variability, identification and modeling of the dominant parameters, together with experimental measurement on a current graphite-aluminum composite. The statistical strength of several graphite spools are measured by testing single filament specimens at the beginning and at the end of the spools, thereby characterizing the statistical parameters associated with the strength variability among the spools and within each spool. The graphite-aluminum wire, produced from continuous liquid infiltration process are tested in tension. The metal matrix composite statistical strengths from different spools are compared with the respective statistical strength of the parent fiber. The results suggest that, given proper interpretation, single filament fiber strength is a sensitive parameter for quality assurance of metal matrix composites.

U.S. Army Materials Technology Laboratory, Watertown, Massachusetts 02172-0001
STATISTICAL STRENGTH COMPARISON OF METAL-MATRIX AND POLYMERIC-MATRIX COMPOSITES -
Edward M. Wu and Shun-Chin Chou

Technical Report MTL TR 89-30, April 1989, 19 pp - illus-tables, D/A Project 536-6010 P62322. K14A-2585, AMCMS Code 69200R.897 A050

AD ____________

UNCLASSIFIED
UNLIMITED DISTRIBUTION

Key Words

Statistical strength
Dimensional scaling
Size effect

The reliability of a composite structure depends on the materials strength variability. Unidirectional composites fail sequentially initiating from the very weakest fiber sites with matrix binder providing local redundancy by transferring load to neighboring fibers until cumulation and clustering of these sites lead to severe stress concentration and ultimate structure failure. As a consequence, the variability of the metal matrix structure is traceable to the strength variability of the constituent fiber, the metal matrix coating process, and the composite wire consolidation process. This report focuses on the partitioning of the first two sources of variability, identification and modeling of the dominant parameters, together with experimental measurement on a current graphite-aluminum composite. The statistical strength of several graphite spools are measured by testing single filament specimens at the beginning and at the end of the spools, thereby characterizing the statistical parameters associated with the strength variability among the spools and within each spool. The graphite-aluminum wire, produced from continuous liquid infiltration process are tested in tension. The metal matrix composite statistical strengths from different spools are compared with the respective statistical strength of the parent fiber. The results suggest that, given proper interpretation, single filament fiber strength is a sensitive parameter for quality assurance of metal matrix composites.

U.S. Army Materials Technology Laboratory, Watertown, Massachusetts 02172-0001
STATISTICAL STRENGTH COMPARISON OF METAL-MATRIX AND POLYMERIC-MATRIX COMPOSITES -
Edward M. Wu and Shun-Chin Chou

Technical Report MTL TR 89-30, April 1989, 19 pp - illus-tables, D/A Project 536-6010 P62322. K14A-2585, AMCMS Code 69200R.897 A050

AD ____________

UNCLASSIFIED
UNLIMITED DISTRIBUTION

Key Words

Statistical strength
Dimensional scaling
Size effect

The reliability of a composite structure depends on the materials strength variability. Unidirectional composites fail sequentially initiating from the very weakest fiber sites with matrix binder providing local redundancy by transferring load to neighboring fibers until cumulation and clustering of these sites lead to severe stress concentration and ultimate structure failure. As a consequence, the variability of the metal matrix structure is traceable to the strength variability of the constituent fiber, the metal matrix coating process, and the composite wire consolidation process. This report focuses on the partitioning of the first two sources of variability, identification and modeling of the dominant parameters, together with experimental measurement on a current graphite-aluminum composite. The statistical strength of several graphite spools are measured by testing single filament specimens at the beginning and at the end of the spools, thereby characterizing the statistical parameters associated with the strength variability among the spools and within each spool. The graphite-aluminum wire, produced from continuous liquid infiltration process are tested in tension. The metal matrix composite statistical strengths from different spools are compared with the respective statistical strength of the parent fiber. The results suggest that, given proper interpretation, single filament fiber strength is a sensitive parameter for quality assurance of metal matrix composites.

U.S. Army Materials Technology Laboratory, Watertown, Massachusetts 02172-0001
STATISTICAL STRENGTH COMPARISON OF METAL-MATRIX AND POLYMERIC-MATRIX COMPOSITES -
Edward M. Wu and Shun-Chin Chou

Technical Report MTL TR 89-30, April 1989, 19 pp - illus-tables, D/A Project 536-6010 P62322. K14A-2585, AMCMS Code 69200R.897 A050

AD ____________

UNCLASSIFIED
UNLIMITED DISTRIBUTION

Key Words

Statistical strength
Dimensional scaling
Size effect

The reliability of a composite structure depends on the materials strength variability. Unidirectional composites fail sequentially initiating from the very weakest fiber sites with matrix binder providing local redundancy by transferring load to neighboring fibers until cumulation and clustering of these sites lead to severe stress concentration and ultimate structure failure. As a consequence, the variability of the metal matrix structure is traceable to the strength variability of the constituent fiber, the metal matrix coating process, and the composite wire consolidation process. This report focuses on the partitioning of the first two sources of variability, identification and modeling of the dominant parameters, together with experimental measurement on a current graphite-aluminum composite. The statistical strength or several graphite spools are measured by testing single filament specimens at the beginning and at the end of the spools, thereby characterizing the statistical parameters associated with the strength variability among the spools and within each spool. The graphite-aluminum wire, produced from continuous liquid infiltration process are tested in tensio . The metal matrix composite statistical strengths from different spools are compared with the respective statistical strength of the parent fiber. The results suggest that, given proper interpretation, single filament fiber strength is a sensitive parameter for quality assurance of metal matrix composites.